Laser Ultrasonic Imaging for Impact Damage Visualization in Composite Structure

Chao Zhang, Jinhao Qiu, Hongli Ji

LASER ULTRASONIC IMAGING FOR IMPACT DAMAGE VISUALIZATION IN COMPOSITE STRUCTURE

Chao Zhang[1], Jinhao Qiu[1*], Hongli Ji[1]

[1] *State Key Laboratory of Mechanics and Control of Mechanical Structures, Nanjing University of Aeronautics and Astronautics, Nanjing 210016, China*

qiu@nuaa.edu.cn

ABSTRACT

Laser ultrasonic scanning technique has great potential for damage evaluation in various applications. In order to detect the size and shape of the damage from the wave propagation information, this paper presents an improved imaging method based on the anomalous incident wave (AIW) energy. Compared with the original wavefield, the AIW filters the reflected wave by using wavenumber-frequency domain analysis and eliminates the traveling waves by means of adjacent incident waves subtraction. Taking these advantages of proposed method, the changes in wave energy distribution caused by the damage can be highlighted to show the size and shape of the damage. Finally, a carbon fibre reinforced polymer (CFRP) laminated plate with an impact damage is used to validate the proposed method. From the result, the proposed method improves the resolution of the damage evaluation.

KEYWORDS : *impact damage, CFRP laminated plate, laser ultrasonic scanning technique, dmage evalutaion.*

INTRODUCTION

In recent decades, composite materials such as carbon fibre reinforced polymer (CFRP) are increasingly used in many engineering fields [1,2]. Their advantages include high stiffness, high specific strength, corrosion resistance and fatigue resistance. However, the damages caused by low-velocity impacts threaten the safety and reliability of structures [3]. Thus, many quantitative non-destructive evaluation (NDE) techniques to detect possible damages have been studied [4-7]. So far, Lamb waves based NDE techniques [8,9] are widely used in plate-like structures, due to their advantages such as high sensitivity to many damage types, long transmission distance and so on. Generally, Lamb waves are generated and received by piezoelectric sensor pairs which are distributed over the inspection region. By using the time-of-flight information of the scattered waves or characteristics of the response signals, the damage position can be detected. However, most of these methods need the signals in 'health' situation as the baselines and a large amount of piezoelectric sensors to improve the inspection quality.

To deal with these problems, ultrasonic propagation visualization method based on a laser ultrasonic scanning technique has been recently developed [10-13]. By using a fixed-point acoustic emission (AE) sensor to collect the ultrasonic waves which are generated by a movable pulse laser, this method provides a series of snapshots to display the ultrasonic waves propagating from a fixed point to an inspection region. By observing the wave propagation, damages can be detected where the anomalous waves occur. To highlight the anomalous waves, many signal processing methods have been proposed such as frequency-wavenumber domain filtering [14-16], wavelet transform[13], anomalous wave propagation [17-19] and so on. However, these works cannot avoid the tedious process in watching the wave propagation frame by frame.

Many imaging methods have been developed to evaluate the damages automated by a digital intensity image. The simplest method is based on the wave energy map [20]. In this method, the wave energy is calculated by the sum of squared signals. And the wave energy at different scanned

points forms an intensity map to represent the energy propagation from the source point. Then, the damage can be shown where the energy declines or gathers. However, the influence of the incident and reflected waves caused by damages affects the wave energy distribution not only in the damage area but also in the large area near the damage. It reduces the resolution of the damage image. Even though the resolution can be improved by increasing the number of the fixed sensors [20], it is necessary to study the signal processing method in damage feature extraction. This paper presents an improved imaging method to identify the damage from the data obtained by one fixed sensor. Both frequency-wavenumber domain filtering and anomalous wave calculation are used to construct the anomalous incident wave (AIW) energy map. And a CFRP laminated plate with an impact damage is experimentally evaluated to validate the proposed method.

1   LASER ULTRASONIC SCANNING TECHNIQUE

As shown in Figure 1, the laser ultrasonic scanning technique includes a laser generator to generate the ultrasonic waves and an AE sensor to obtain the ultrasonic signal. By scanning the laser point over the inspection region through a two-dimensional laser scanning mirror, the response signals between the different laser points and the fixed sensor point can be obtained. Based on the reciprocal theorem in elastodynamics [21,22], these obtained signals are converted to represent the ultrasonic waves propagating from the sensor point to the inspection region. Thus, the responses of each scanning points at the same time t are plotted on an intensity snapshot to represent the wavefield at the time point t. Finally, the snapshots are continually displayed in a time series and show the wave propagation in the inspection region.
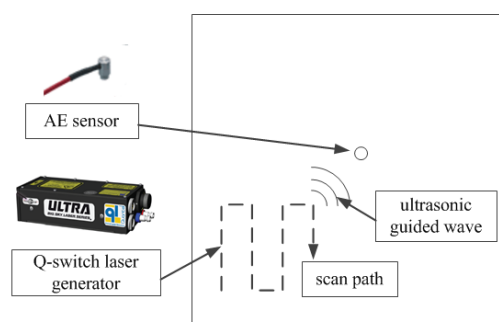

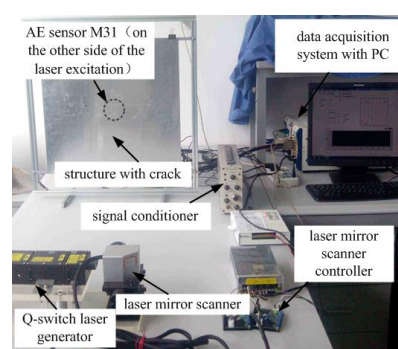Figure 1: Schematic diagram of ultrasonic propagation visualization

Figure 2: Experimental setup of laser ultrasonic scanning technique

According to the principle of laser ultrasonic scanning technique, the experimental system is developed as shown in Figure 2. The following main devices are used: a lamp-pumped pulse Nd: YAG laser (Ultra-100, Quantel corp., USA), a two-dimensional laser mirror scanner (TSH8203H, Century Sunny corp., China), a micro-miniature AE sensor (M31, Fuji Ceramics corp., Japan), a pre-amplifier (A1002, Fuji Ceramics corp., Japan) and an AE analyser (AE9922, NF corp., Japan). The laser mirror is controlled by an analog output module (cRIO-9263, NI corp., USA) and the signals are sampled by a high-speed digitizer (PXI-5105, NI corp., USA). All the devices are synchronized by a controller (PXIe-8133, NI corp., USA).

2   CFRP LAMINATED PLATE WITH AN IMPACT DAMAGE

A symmetric CFRP laminated plate with a stacking configuration of $[45°/-45°/0°/90°]_s$ is used to validate the damage evaluation method. The dimensions of the CFRP plate are $480 \times 480 mm^2$ and the thickness is 1mm. To make an artificial damage, a drop-weight impact test is performed according to Test Method D7136 [23]. Damage is imparted through out-of-plane, concentrated

impact (perpendicular to the plane of the CFRP plate) using a drop weight with a hemispherical striker tip as shown in Figure 3. The impact energy E_{impact} can be calculated by:

$$E_{impact} = mgh \tag{1}$$

where m is the mass of the drop weight, g is the acceleration due to gravity and h is the drop-height. In this paper, the impact energy is 10J and the impact damage is shown in Figure 4. The damage is difficultly to be detected visually. However, the delamination, split and crack exist inside the structure.
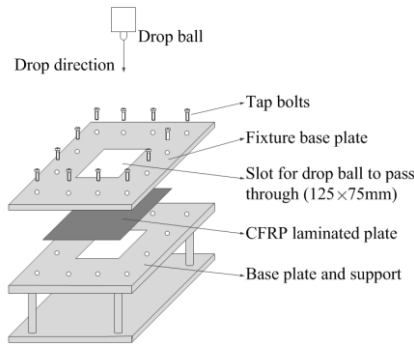

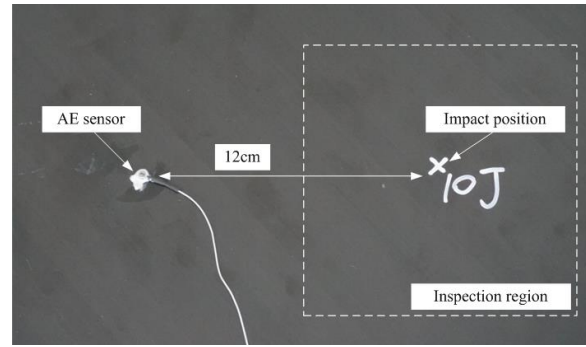Figure 3: Schematic diagram of the drop-weight impact test for a CFRP plate

Figure 4: Picture of the CFRP plate with a damage caused by a 10J impact

3   DAMAGE EVALUATION USING AIW ENERGY MAP

As shown in Figure 4, the impacted side of the CFRP laminated plate is scanned by the movable laser point and the inspection region is $100\times100\text{mm}^2$. The AE sensor is placed on the opposite side of the CFRP plate with a distance 12cm away from the centre of inspection region. Due to the spatial interval is 1mm, 10201 points are scanned which costs 8.5min at the max laser repeat frequency 20Hz. The signal is filtered with the band-pass frequency from 100kHz to 200kHz. To obtain the waves propagating though the inspection region, the sampling period is set as 200μs and the sampling frequency is 10MS/s.
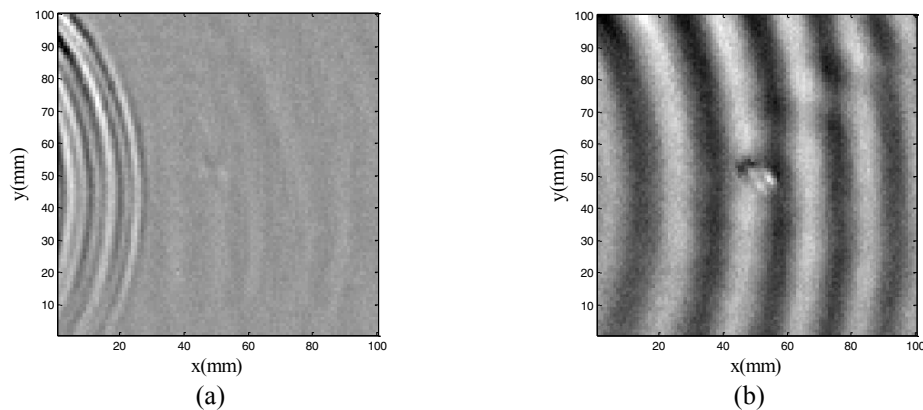

(a)   (b)

Figure 5. Experimental wavefields at different times: (a) $t=60$μs; (b) $t=160$μs

3.1   Ultrasonic propagation visulization

The wavefields at different times can be obtained by a series of snapshots whose intensity values equal to the voltage responses at different laser points. As shown in Figure 5(a), the waves propagate from the source to the inspection region and only A_0 waves can be seen due to the amplitude of S_0 mode waves is much smaller. After about 160μs as shown in Figure 5(b), the A0

mode waves pass through the impact damage. And the amplitude changes around the damage region which can detect the position of the damage. However, the size and shape cannot be identified due to the complex wave propagation in damage region.

3.2   Wave energy map

Wave energy map is usually used to evaluate the damage as present in [20]. As the definition of signal energy in digital signal processing, the wave energy $E(x, y)$ obtained at the position (x, y) can be calculated by:

$$E(x,y) = \sum_{i=1}^{N} v^2(i,x,y) \tag{2}$$

where $v(i, x, y)$ is the response of the AE sensor, i represents the time variable and N represents the sampling length. Due to that the wave propagation in the structure can be regard as the energy propagation from the source point. The wave energy map which represents the distribution of the wave energy will be uniform in the continuous structure. Thus, the anomalous energy region in wave energy map which indicates the waves propagate through the discontinuity should be the damage area.

As shown in Figure 6, the wave energy decreases as the wave propagating. And the anomalous wave energy region shows the impact damage faintly. In order to evaluate the inspection result, Figure 7 shows the damage image obtained by a conventional immersion ultrasonic C-scan method. Compared with Figure 7, the large amount of the wave energy in the 'health' area reduces the resolution of damage image in Figure 6.
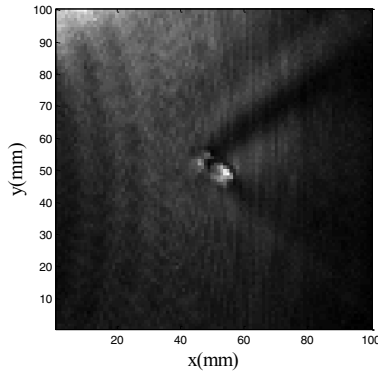

Figure 6. Damage evaluation using the original wave energy map
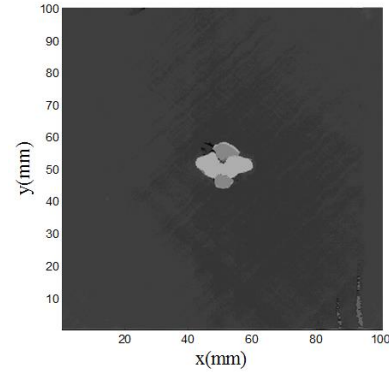
Figure 7. Damage evaluation using immersion ultrasonic C-scan method

3.3   Anomalouse wave propagation method

Anomalous wave propagation [17] can be calculated by adjacent waves subtraction after arrival time matching. Assume the two adjacent signals $v(i, x, y)$ and $v(i, x+\Delta x, y)$, the anomalous wave at the position (x, y) can be defined as:

$$\Delta v(i,x,y) = v(i,x,y) - v(i+d_{r\max}, x+\Delta x, y) \tag{3}$$

where Δx represents the minimum spatial resolution in direction x and the time-lag $d_{r\max}$ can be calculated through the cross-correlation $r(d)$:

$$r(d) = \sum_{i=0}^{N} v(i,x,y) v(i+d, x+\Delta x, y) \tag{4}$$

And $d_{r\max}$ represents the time-lag which makes $r(d_{r\max})$ reach the maximum. Considering that the waves propagate in the continuous medium, two adjacent waves are similar with each other and the time-lag $d_{r\max}$ is the traveling time that waves propagate from (x, y) to $(x+\Delta x, y)$. By adjacent waves

subtraction after arrival time matching, the major component of the traveling wave will be eliminated. And the changes in the waveform caused by the damage can be magnified.

The anomalous wave energy is calculated by:

$$E_{AW}(x,y) = \sum_{i=1}^{N} \Delta v^2(i,x,y) \tag{5}$$

Compared with Figure 6, Figure 8 shows the impact damage size and shape by using the energy distribution of the anomalous waves. However, due to the incident waves are much stronger than the reflected waves, the time-lag $d_{r\,max}$ only denotes the time delay of the incident waves. Because the reflected waves and incident waves have the opposite time delays between adjacent points, the reflected waves are also enlarged by adjacent waves subtraction which also reduces the resolution of damage image.
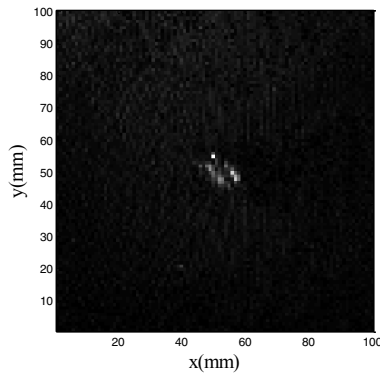

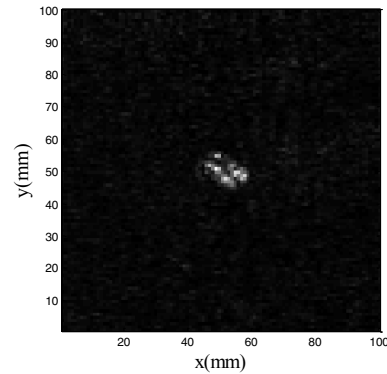Figure 8. Damage evaluation using the anomalous wave energy map

Figure 9. Damage evaluation using the AIW energy map

3.4 Frequency-wavenumber domain filtering

To improve the resolution of the damage image further and eliminate the influence of the reflected wave in anomalous wave calculation, frequency-wavenumber domain analysis is used in this paper to filter the reflected wave. As presented in [14], three-dimensional Fourier transform (3D-FT) converts the wavefield from time-space (t-x-y) domain into frequency-wavenumber (ω-k_x-k_y) domain. The process of 3D-FT can be given by:

$$V(\omega, k_x, k_y) = \int_{-\infty}^{+\infty} \int_{-\infty}^{+\infty} \int_{-\infty}^{+\infty} v(t,x,y) e^{-j(\omega t + k_x x + k_y y)} dt dx dy \tag{6}$$

where k_x and k_y are the wavenumber, ω is the angular frequency, j is the imaginary unit and $V(\omega, k_x, k_y)$ is wavefield in frequency-wavenumber domain, while $v(t, x, y)$ is wavefield in time-space domain. Considering that the wave source is on the left of the inspection region, the incident waves propagate along the positive x direction and the reflected waves are along the negative x direction. Thus, the wavefield in frequency-wavenumber domain can be divided into two parts: incident wave portion which is in the quadrant with $k_x\omega<0$; reflected wave portion which is in the quadrant with $k_x\omega>0$. And then, the reflected waves can be removed by adding a window function Φ_I:

$$\Phi_I = \begin{cases} 0 & k_x\omega \geq 0 \\ 1 & k_x\omega < 0 \end{cases} \tag{7}$$

Finally, the incident waves in time-space domain can be obtained through three-dimensional inverse Fourier transform (3D-IFT):

$$v_I(t,x,y) = \frac{1}{2\pi} \int_{-\infty}^{+\infty} \int_{-\infty}^{+\infty} \int_{-\infty}^{+\infty} V(\omega, k_x, k_y) \Phi_I e^{j(\omega t + k_x x + k_y y)} d\omega dk_x dk_y \tag{8}$$

In addition, the ultrasonic signals in this paper are collected by a digital acquisition, the wavefield data is discrete data. Thus, the Fourier transform is achieved by fast Fourier transform (FFT).

After filtering the reflected wave, the AIW can be obtained as equation (3) with the incident wavefield $v_I(i, x, y)$ instead of $v(i, x, y)$. Compared with calculating anomalous wave directly from the original wavefield, AIW not only extracts the wave propagation changes caused by the impact damage, but also removes the negative influence from the reflected waves in matching the arrival times of two adjacent waves. Figure 9 shows the damage evaluation result using AIW energy map. Compared with Figure 8, the resolution in Figure 9 is improved which the shape and size of the impact damage is much clearer.

CONCLUSION

This paper presents a novel imaging method for damage visualization based on laser ultrasonic scanning technique. In this method, the incident wavefield is separated from the original wavefield by frequency-wavenumber domain filtering. And then, AIW is calculated by adjacent incident waves subtraction after arrival time matching. Finally, the AIW energy map is constructed to show the size and shape of the damage. To validate the proposed method, a CFRP laminated plate with an impact damage is evaluated experimentally. Compared with the damage imaging using the energy distribution map of original waves and anomalous waves, the AIW energy map improve the resolution of the results. In addition, a further study is also warranted to extend the present study for actual damage detection in more complex and practical structure.

ACKNOWLEDGMENTS

REFERENCES

[1] C. Soutis. Fibre reinforced composites in aircraft construction. *Progress in Aerospace Sciences* 41 (2) (2005) 143-151.

[2] L. Ye, Y. Lu, Z. Su, G. Meng. Functionalized composite structures for new generation airframes: a review. *Composites Science and Technology* 65 (9) (2005) 1436-1446.

[3] M. Sultan, K. Worden, W. Staszewski, A. Hodzic. Impact damage characterisation of composite laminates using a statistical approach. *Composites Science and Technology* 72 (10) (2012) 1108-1120.

[4] B.W. Drinkwater, P.D. Wilcox. Ultrasonic arrays for non-destructive evaluation: A review. *NDT & E International* 39 (7) (2006) 525-541.

[5] D. Bull, L. Helfen, I. Sinclair, S. Spearing, T. Baumbach. A comparison of multi-scale 3D X-ray tomographic inspection techniques for assessing carbon fibre composite impact damage. *Composites Science and Technology* 75 (2013) 55-61.

[6] J. Cheng, H. Ji, J. Qiu, T. Takagi, T. Uchimoto, N. Hu. Novel electromagnetic modeling approach of carbon fiber-reinforced polymer laminate for calculation of eddy currents and eddy current testing signals. *Journal of Composite Materials* (2014) 0021998314521475.

[7] A. Maier, R. Schmidt, B. Oswald-Tranta, R. Schledjewski. Non-Destructive Thermography Analysis of Impact Damage on Large-Scale CFRP Automotive Parts. *Materials* 7 (1) (2014) 413-429.

[8] J.E. Michaels. Detection, localization and characterization of damage in plates with an in situ array of spatially distributed ultrasonic sensors. *Smart Materials and Structures* 17 (3) (2008) 035035.

[9] V. Giurgiutiu. Embedded NDT with Piezoelectric Wafer Active Sensors. *Nondestructive Testing of Materials and Structures* 2013, pp. 987-992.

[10] J. Takatsubo, B. Wang, H. Tsuda, N. Toyama. Generation laser scanning method for the visualization of ultrasounds propagating on a 3-D object with an arbitrary shape. *Journal of Solid Mechanics and Materials Engineering* 1 (2007) 1405-1411.

[11] S. Yashiro, J. Takatsubo, N. Toyama. An NDT technique for composite structures using visualized Lamb-wave propagation. *Composites Science and Technology* 67 (15) (2007) 3202-3208.

[12] J.-R. Lee, H. Jeong, C.C. Ciang, D.-J. Yoon, S.-S. Lee. Application of ultrasonic wave propagation imaging method to automatic damage visualization of nuclear power plant pipeline. *Nuclear engineering and design* 240 (10) (2010) 3513-3520.

[13] J.-R. Lee, S.Y. Chong, N. Sunuwar, C.Y. Park. Repeat scanning technology for laser ultrasonic propagation imaging. *Measurement Science and Technology* 24 (8) (2013) 085201.

[14] M. Ruzzene. Frequency–wavenumber domain filtering for improved damage visualization. *Smart Materials and Structures* 16 (6) (2007) 2116.

[15] Y.-K. An, B. Park, H. Sohn. Complete noncontact laser ultrasonic imaging for automated crack visualization in a plate. *Smart Materials and Structures* 22 (2) (2013) 025022.

[16] H. Sohn, D. Dutta, J. Yang, M. DeSimio, S. Olson, E. Swenson. Automated detection of delamination and disbond from wavefield images obtained using a scanning laser vibrometer. *Smart Materials and Structures* 20 (4) (2011) 045017.

[17] J.-R. Lee, C. Ciang Chia, C.-Y. Park, H. Jeong. Laser ultrasonic anomalous wave propagation imaging method with adjacent wave subtraction: Algorithm. *Optics & Laser Technology* 44 (5) (2012) 1507-1515.

[18] C.C. Chia, J.-R. Lee, C.-Y. Park, H.-M. Jeong. Laser ultrasonic anomalous wave propagation imaging method with adjacent wave subtraction: application to actual damages in composite wing. *Optics & Laser Technology* 44 (2) (2012) 428-440.

[19] Z.M. Master, T.E. Michaels, J.E. Michaels. Incident wave removal for defect enhancement in acoustic wavefield imaging. *AIP conference Proceedings*, Vol. 894, IOP INSTITUTE OF PHYSICS PUBLISHING LTD, 2007, p. 665.

[20] Y. Liu, N. Hu, H. Xu, W. Yuan, C. Yan, Y. Li, R. Goda, J. Qiu, H. Ning, L. Wu. Damage Evaluation Based on a Wave Energy Flow Map Using Multiple PZT Sensors. *Sensors* 14 (2) (2014) 1902-1917.

[21] M. Fink, C. Prada. Acoustic time-reversal mirrors. *Inverse problems* 17 (1) (2001) R1.

[22] J.D. Achenbach. *Reciprocity in elastodynamics*. Cambridge University Press, 2003.

[23] A. Standard, D7136/D7136M–05, Standard test method for measuring the damage resistance of a fiber-reinforced polymer matrix composite to a drop-weight impact event. West Conshohocken (PA): ASTM International (2005).